Viscoelasticity of Epoxy Resin/Silica Hybrid Materials with an Acid Anhydride Curing Agent

Wakako Araki, Shogo Wada, Tadaharu Adachi

Department of Mechanical Sciences and Engineering, Tokyo Institute of Technology, 2-12-1 O-Okayama, Meguro-Ku, Tokyo 152-8552 Japan

Received 15 October 2007; accepted 20 December 2007
DOI 10.1002/app.27887
Published online 19 February 2008 in Wiley InterScience (www.interscience.wiley.com).

ABSTRACT: The viscoelasticity of epoxy resin/silica hybrid materials manufactured by the sol–gel process with an acid anhydride curing agent was investigated in terms of morphology. Transmission microscopy observations demonstrated that all the prepared hybrid samples had a two-phased structure consisting of an epoxy phase and a silica phase. The formed silica had either nanosized particles or coarse domains, depending on the catalyst for the sol–gel process. Raman spectroscopy analysis showed that the formed silica had features typical of sol–gel derived silica glass and that the ring-opening reactions of the epoxy groups developed in the hybrid samples and in the neat epoxy samples. In dynamic mechanical thermal analysis, there were two transition temperatures due to epoxy chain mobility and epoxy network relaxation, through which the moduli changed by nearly 3 orders of magnitude. The hybridization disturbed epoxy network formation but also reinforced the epoxy network with the formed silica, which was characterized by the activation energy of the network relaxation; therefore, the modulus of the rubbery state was correlated to the activation energy. © 2008 Wiley Periodicals, Inc. J Appl Polym Sci 108: 2421–2427, 2008

Key words: composites; morphology; viscoelastic properties

INTRODUCTION

Organic/inorganic hybrid materials have been of great interest in various fields and are expected to have novel properties because they have both organic and inorganic phases blended in a nanometer order and/or on a molecular level. The most common process for incorporating an inorganic phase into an organic phase is a sol–gel process using metal alkoxides, such as tetraethoxysilane (TEOS), that produces an inorganic phase through two reactions: hydrolysis and polycondensation. The sol–gel process has been used with many organic polymers[1–22] to produce organic/inorganic hybrid materials.

Several researchers have worked on hybrid materials that are based on epoxy resins[11–22] and prepared by the sol–gel process. These researchers have reported significant improvements in material properties such as high thermal stability and high glass-transition temperatures. We reported an improvement in the dynamic modulus and a prediction model for the modulus of epoxy resin/silica hybrid materials in our previous study.[23]

Generally, amine or acid anhydride curing agents are used for a neat epoxy system; however, most research on hybrid materials with an epoxy resin base has been done with amine curing agents, whereas little research has been reported on materials that include acid anhydride curing agents. Mascia and Tang[24] investigated organic/inorganic hybrid materials, using an epoxy resin functionalized with an organotrialkoxysilane consisting of methyl nadic anhydride. As for the glass-transition temperature, they concluded that hybridization interfered with the crosslinking reaction because of the curing agent, resulting in a reduction in the glass-transition temperature of the epoxy resin. Fujiwara et al.[25] investigated various epoxy hybrid systems including hexahydrophthalic anhydride. They also reported a decrease in the glass-transition temperature as well as a loss of the glass-transition temperature caused by hybridization. In addition, no research from a mechanical point of view has been done on the viscoelasticity of hybrid materials that include an acid anhydride.

In this study, the effect of hybridization on the morphology and viscoelasticity of epoxy resin/silica materials prepared via the sol–gel process with an acid phthalic anhydride curing agent was investigated, with a particular focus on the effect of the formation of the epoxy phase and the silica phase on the dynamic modulus. Epoxy resin/silica hybrid samples were prepared with and without a catalyst for the sol–gel process to examine the effects of the acid anhydride curing agent as a catalyst. The morphology of the organic and inorganic phases of the

Correspondence to: W. Araki (araki@mech.titech.ac.jp).

TABLE I
Mixture Ratio (w/w) for Sample Preparation

Sample		DGEBA	MeTHPA	HD-Acc43	TEOS	H_2O	HCl	IPA
Epoxy		100	80	0.5	0	0	0	0
HybA	A1	100	80	0.5	7.84	2.03	0	15
	A2	100	80	0.5	15.7	4.06	0	15
	A3	100	80	0.5	31.3	8.12	0	15
HybB	B1	100	80	0.5	7.84	2.03	0.12	15
	B2	100	80	0.5	15.7	4.06	0.12	15
	B3	100	80	0.5	31.3	8.12	0.12	15
HybC	C2	100	80	0.5	15.7	4.06	1.4	200

prepared hybrid samples was observed with transmission electron microscopy (TEM) and micro-Raman spectroscopy. Viscoelastic properties were examined by dynamic mechanical thermal analysis and are discussed on the basis of the results of the morphology observations.

EXPERIMENTAL

Sample preparation

Diglycidyl ether of bisphenol A (DGEBA) epoxy resin (DER331, Dow Chemical), 3,4-methyl-1,2,3,6-tetrahydrophthalic anhydride (MeTHPA; HN-2200R, Hitachi Chemical, Tokyo, Japan) as a curing agent, and 2,4,6-tris (dimethylaminomethyl) phenol as an accelerator (Daitocurar HD-Acc43, Daito Sangyo, Osaka, Japan) were used as organic components. The weight ratio of the resin, curing agent, and accelerator was 100 : 80 : 0.5.

To form an inorganic phase in the organic matrix during the sol–gel process, TEOS (KBE-04, Shin-Etsu Chemical, Tokyo, Japan) as an alkoxyl silane, hydrochloride (HCl) as a catalyst, isopropyl alcohol (IPA) as a solvent, and water (H_2O) were used in various mixture ratios. The molar ratio of H_2O to TEOS was 3 : 1, and HCl was added to adjust the pH of the entire mixture to 2–3. The weight ratio of IPA to DGEBA was either 0.15 or 2.0. The mixture ratios of the samples are summarized in Table I.

For the neat epoxy sample, which is called Epoxy hereafter, the organic raw materials were mixed, agitated, cast, and degassed *in vacuo* and then were cured under fixed curing conditions: at 353 K for 3 h and then at 413 K for 15 h in a thermostatic oven (WFO-450PD, Tokyo Rikakikai, Tokyo, Japan).

To manufacture the epoxy resin/silica hybrid sample called HybA hereafter, TEOS was hydrolyzed at room temperature for 1 h after being blended with IPA and H_2O. Then, the organic raw materials were blended in this TEOS mixture with various ratios of DGEBA to TEOS until the mixture became transparent. After that, the mixture was cast and cured in the thermostatic oven with the same curing process used to form Epoxy, and this was followed by an additional curing process at 413 K for 24 h to complete the curing of the epoxy resin and also polycondensation for the sol–gel reaction.

The hybrid sample called HybB was made with HCl as a catalyst in the hydrolysis process to determine if MeTHPA could function as a catalyst in the sol–gel process in comparison with HybA. The process after the hydrolysis of HybB was the same as that of HybA. The other hybrid sample, called HybC, was made with a large amount of IPA to obtain thoroughly homogeneous samples with a well-dispersed inorganic phase. The mixture was kept at room temperature for a few days, and this was followed by the same curing processes used to make HybA and HybB.

Experiments

To evaluate the content of the silica phase formed in the hybrid samples, the specimens were placed in a furnace (Muffle Furnace MC FP31, Yamato Scientific, Tokyo, Japan) at 1073 K for 6 h to pyrolyze the epoxy phase. The weights of each sample before and after the pyrolysis were measured.

The hybrid samples were observed with a transmission electron microscope (JEM-200CX, JEOL, Tokyo, Japan) to investigate their morphology. The samples observed with TEM were prepared with an ultramicrotoming machine (Ultracut-N, Reichert, NY) and cut to a thickness of about 60 nm with a diamond knife. An accelerating voltage of 80 kV was used.

Raman spectroscopy analysis was performed with a laser micro-Raman spectrometer (NRS-1000, Jasco, Tokyo, Japan). A green laser with a wavelength of 532.3 nm and a power of 100 mW was used, and the spectral slit was 50 μm wide. The space resolution was 2 μm, and the exposure time was less than 120 s. The epoxy phase and also the inorganic phase of the hybrid samples obtained by the dissolution of the epoxy phase with sulfuric acid were investigated.

A dynamic mechanical thermal analysis (Tritec 2000, Triton Technology, Lincolnshire, UK) was performed to measure the dynamic modulus, mechanical

TABLE II
Appearance and Silica Content

Sample		Appearance	Silica content ϕ, wt %	Remarks
Epoxy		Transparent	0	
HybA	A1	Transparent (sparsely translucent)	1.0	
	A2		2.4	
	A3		—	Voids
HybB	B1	Opaque	0.8	
	B2		3.0	
	B3		—	Voids
HybC	C2	Transparent	3.2	Wrinkles and cracks

loss, and glass-transition temperature. The bending mode (or single-cantilever clamping mode) and shear mode were used. The test frequencies of 1, 3.16, and 10 Hz were used, and the temperature range was 290–450 K with an increasing rate of 2 K/min for the bending mode and 4 K/min for the shear mode.

RESULTS AND DISCUSSION

Content and size of the formed silica

Table II summarizes the appearance of the samples and the silica content. Epoxy was yellowish and transparent. The HybA samples were also yellowish and transparent and sparsely translucent. The HybB samples were yellowish and homogeneously opaque. HybC was transparent like Epoxy; it is possible that nanosized and/or smaller silica phases formed, although it was wrinkled and cracked because of the shrinkage during the drying and curing processes.

For all the hybrid samples, the silica content was about 3 wt % as the ratio of TEOS to DGEBA increased to 15.7 wt %. The HybA and HybB samples with a high TEOS content of 31.3 wt % contained many voids because of the evaporation of IPA and ethanol, a byproduct of the sol–gel reaction during the curing process. There were no apparent differences between the silica contents of HybA and HybB, regardless of the catalyst used.

Figure 1(a) shows TEM pictures of HybA2 and HybB2. All the hybrid samples were found to be two-phased in structure: the epoxy phase and the silica phase. In HybA, small silica particles that were smaller than 100 nm and their agglomerations were dispersed in the clear epoxy phase. On the other hand, in HybB, larger silica domains, several micrometers in size, were present, which made the HybB samples opaque, as previously described. Furthermore, these coarse domains were easily damaged by the microtoming because of their brittleness, whereas the nanosize silica particles were tough.

It was thus demonstrated that the acid anhydride curing agent (MeTHPA) worked as well as the curing agent as a catalyst for the sol–gel reaction. The sample with MeTHPA as the catalyst, in which nanosized silica particles had formed, was generally transparent, whereas the sample with HCl as a catalyst, in which large, brittle silica domains of several micrometers had formed, was opaque. Furthermore, a large amount of IPA as a solvent with HCl made the sample transparent but also made it difficult to manufacture hybrid samples without any shrinkage. Thus, the amounts of the catalyst and solvent greatly affected the size of the formed silica, whereas the silica content depended simply on the TEOS content. The HybA3, HybB3, and HybC2 samples are excluded from the following discussion because of their voids and cracks.

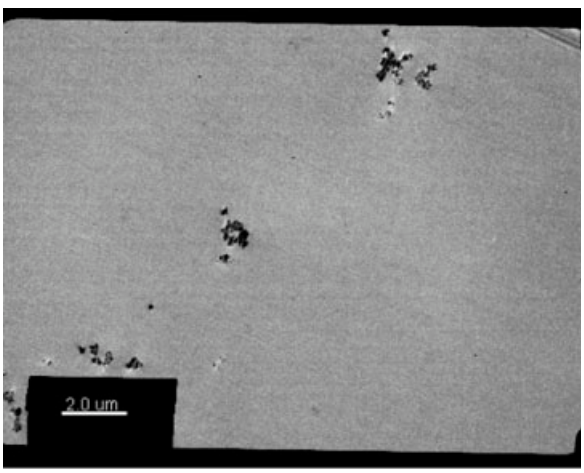

(a) HybA2 (×5000)

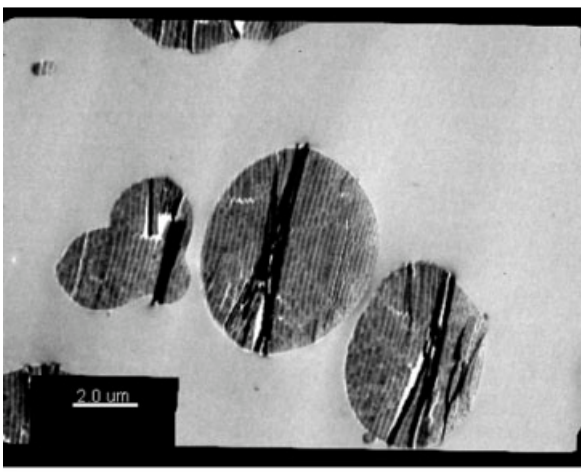

(b) HybB2 (×5000) (damaged by microtoming)

Figure 1 TEM pictures (at a magnification of 5000×).

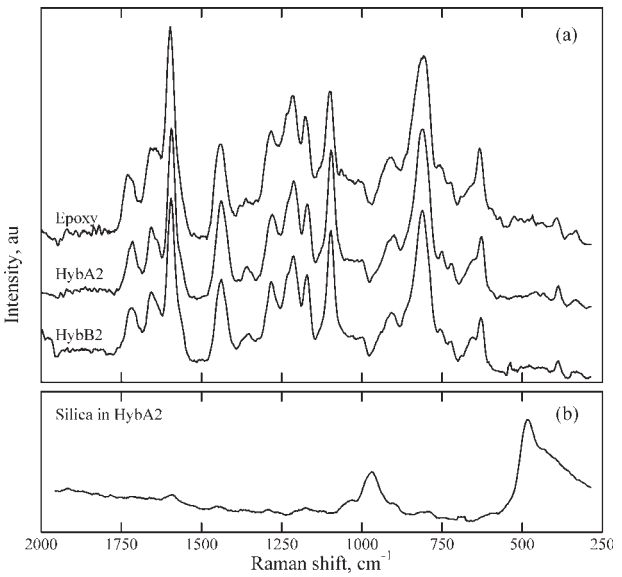

Figure 2 Raman spectra: (a) epoxy phase and (b) silica phase.

Raman spectroscopy analysis

Figures 2(a) shows the Raman spectra of the epoxy phase in Epoxy, HybA2, and HybB2. The spectra between 250 and 2000 cm^{-1} were normalized by the peak intensity of the aromatic ring moiety at 639 cm^{-1}. Common spectra such as vibrations of the hydrocarbon groups between 2800 and 3100 cm^{-1} (not shown here), backbone vibrations related to bisphenol A between 800 and 910 cm^{-1}, and epoxy ring breathing between 1200 and 1300 cm^{-1} were seen for all the samples. There was no particular peak between 2000 and 2500 cm^{-1} or between 3500 and 4500 cm^{-1}.[23]

The spectra of all samples were identical, regardless of the hybridization. The peaks relating to the epoxy groups of the hybrid samples were as small as those of Epoxy, and this demonstrated that the ring-opening reaction proceeded in the hybrid samples as much as in Epoxy. No peaks regarding byproducts or covalent bands between organic and inorganic phases were observed in the hybrid samples.

Figure 2(b) shows the Raman spectrum of the formed silica phase in HybA2. The spectrum shows typical features of silica glass formed with the sol–gel method at a relatively low temperature, such as a very strong peak of four-membered rings at 485 cm^{-1} and Si—OH groups at 970 cm^{-1}; this differed from that of fused amorphous silica.[26,27] The features were common in the silica formed in all the hybrid samples. This spectrum also implies that the formed silica possibly had nanosized (or smaller) porous structures like those of the sol–gel silica glass formed at a low temperature, which could make the large silica domains in HybB brittle.[28,29]

The Raman spectroscopy analysis showed that the ring-opening reaction of the epoxy groups developed in all the hybrid samples as well as Epoxy. The formed silica particles in all the hybrid samples had typical features of sol–gel-derived silica glass, which contained a lot of four-membered rings and Si—OH groups. There were no covalent bonds between these phases.

Dynamic mechanical thermal analysis

Figure 3 shows the dynamic storage modulus and mechanical loss measured at 1 Hz with the bending mode. Epoxy showed the typical viscoelastic behavior: a glassy region, a rubbery region, and a glass transition around 410 K. All the hybrid samples also showed viscoelastic behaviors; however, the two transitions took place at far lower temperatures between 340 and 380 K, at which the moduli plummeted. The moduli above 390 K were too low to be measured with the bending mode.

Figure 4 shows the dynamic shear modulus (G') and mechanical loss measured at 1 Hz. The two transitions were clearly visible in all hybrid samples; one was at about 340 K, and the other one was between 370 and 400 K. Through these two transitions, the

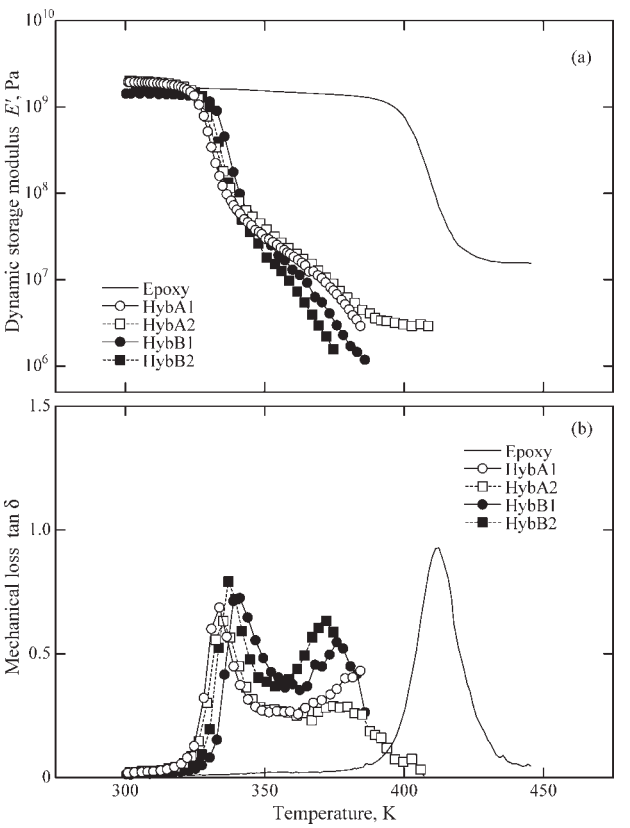

Figure 3 Dynamic mechanical thermal analysis results measured with the bending mode: (a) dynamic storage modulus (E') and (b) mechanical loss (tan δ).

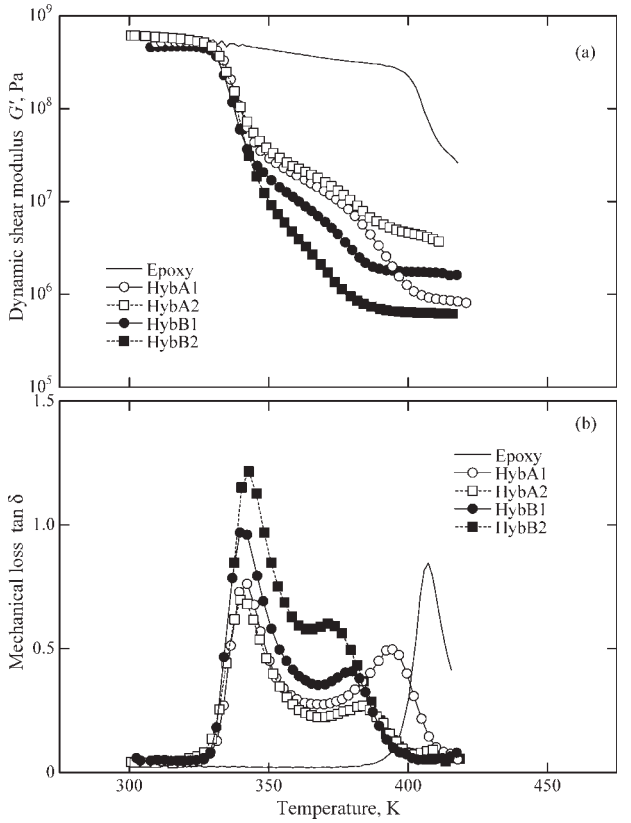

Figure 4 Dynamic mechanical thermal analysis results measured with the shear mode: (a) dynamic shear modulus (G') and (b) mechanical loss (tan δ).

moduli dropped by nearly 3 orders of magnitude and showed the rubbery state around 410 K.

Figure 5(a) shows the relationship between the silica content and the transition temperature, which was defined as the peak temperature of the mechanical loss measured at 1 Hz. The two overlapping peaks in Figure 4 were separately evaluated by Lorentzian curve fitting. The transition at a lower temperature for all hybrid samples took place at 360 K, which was close to the melting temperature of phenoxy resin,[30,31] a thermoplastic resin chemically similar to epoxy resin, so the transition at the lower temperature can be attributed to the mobility of epoxy chain structures. The other transition occurred at different temperatures depending on the sample types. This transition can result from the relaxation of epoxy network structures, so the transition at the higher temperature is considered to be related to the network density.[32,33] The epoxy network became rougher when the silica content increased, and HybB had rougher network structures than HybA.

Figure 5(b) shows the relationship between the silica content and G' of the glassy state at 323 K and the rubbery state at 408 K. G' of the rubbery state of Epoxy was determined with the dynamic storage modulus in Figure 3(a) because it was not obtained with the shear mode. In the glassy state, G' was constant at approximately 0.3 GPa, being independent of the silica content. On the other hand, G' in the rubbery state varied. A high G' value was seen for HybA2, close to that of Epoxy, whereas G' of HybB2 was small, even though they had almost the same silica content of about 3 wt %.

To investigate the epoxy network contributing to G' of the rubbery state, the activation energy of the network relaxation (ΔH) was determined from the dependence of the transition temperatures on the frequency (f), $\Delta H/R = d(\ln f)/d(1/T_g)$ (where R is the gas constant and T_g is the glass-transition temperature), which is represented by the slope in Figure 6(a).[34] The slopes (i.e., ΔH) of HybA2 and B1 were larger than those of HybA1 and B2. Figure 6(b) shows a good correlation between ΔH and G': G' increased with increasing ΔH, regardless of the silica content. The increase of G' along with ΔH could be related to the rigidity of the network. Further discussion is found in the following subsection.

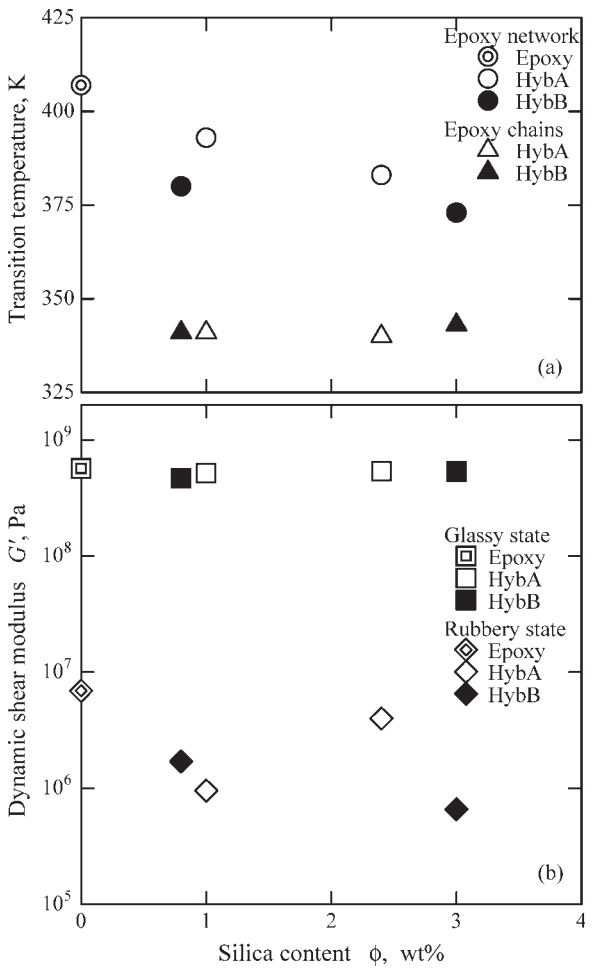

Figure 5 Silica content (φ) and viscoelastic properties: (a) transition temperatures and (b) shear modulus (G') of the rubbery state.

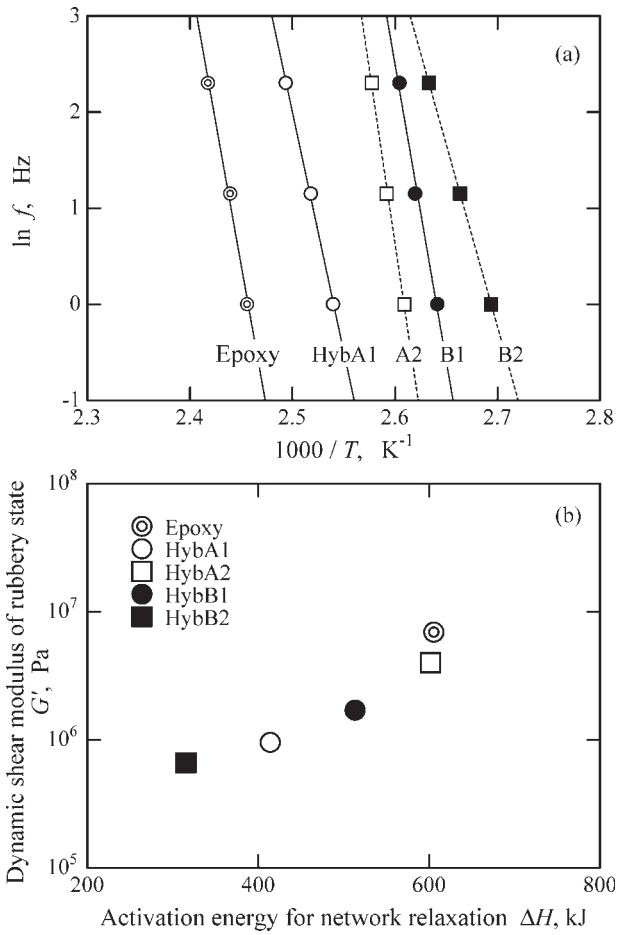

Figure 6 Activation energy of network relaxation (ΔH): (a) dependence of the transition temperature on the frequency (f) and (b) ΔH and shear modulus (G') of the rubbery state.

Discussion of the viscoelasticity in terms of the morphology

In all the HybA and HybB samples, epoxy chain structures formed, and the epoxy network structure became rougher with the increase in the silica content. This probably occurred because the formation of the silica, especially the large domains in HybB, hindered epoxy network formation during the simultaneous sol–gel and curing reactions.

G' of the rubbery state of HybB decreased with the silica content when the activation energy of the network relaxation decreased. This may be simply because the network became rougher and more flexible with the silica content. On the other hand, in HybA, the modulus of the rubbery state increased, even though it had a rougher network. These increases could show that the network became rougher but was reinforced by the nanosized particles at the same time, which were characterized by the activation energy, whereas the coarse silica domains in HybB had no reinforcing effect. As for the glassy state, the moduli were independent of the hybridization because they were less sensitive to the network structure and the silica content in this study was too small to affect the moduli.

The hybrid samples, such as HybA1 and HybB2, having modulus changes of 3 orders of magnitude through the transitions, showed interesting viscoelastic behavior: high moduli at room temperature and very flexible behavior, like that of polymer gels, at a higher temperature. Compared with thermoplastic resins such as phenoxy resin, the hybrid samples in this study could deform at high temperatures without melting, and great transparency was possible. In addition, because silica formation in HybA lowered the transition temperature but reinforced the network, it can be suggested that greater silica content would show a unique property such as a low glass-transition temperature along with a high modulus in the rubbery state.

CONCLUSIONS

The morphology and viscoelasticity of epoxy resin/silica hybrid materials manufactured by the sol–gel process with an acid anhydride curing agent were investigated in this study. Samples with and without HCl as an acid catalyst for the sol–gel reaction with different amounts of TEOS were prepared.

All hybrid samples prepared had a two-phased structure: an epoxy phase and a silica phase. The size of the formed silica depended on the HCl catalyst: there were nanosized particles observed in the samples without the catalyst, whereas those with the catalyst had large, brittle silica domains of several micrometers. The content of the silica increased with the amount of TEOS. This silica formation proved that the acid anhydride curing agent also worked as a catalyst.

The Raman spectroscopy analysis showed that the formed silica had typical features of sol–gel derived silica glass. As for the epoxy phase, the ring-opening reactions of the epoxy groups developed in the hybrid samples and in the neat epoxy samples. There were no covalent bonds between these phases.

In the dynamic mechanical thermal analysis, two transition temperatures were obtained: the transition at a lower temperature was attributed to the mobility of the epoxy chain, and the other one was caused by relaxation of the epoxy network. During these two transitions, the moduli changed by nearly 3 orders of magnitude. The moduli of the glassy state were almost constant, despite the hybridization, whereas the moduli of the rubbery state varied. For the hybrid samples with the HCl catalyst, the modulus of the rubbery state decreased with the silica

content because of the rough network structure, whereas the moduli and also the activation energy for the network relaxation of the samples without the catalyst increased with the increase of the silica content because the network was reinforced by the nanosized particles.

The hybridization disturbed the epoxy network formation, resulting in a decrease in the network density, but it also reinforced the epoxy network with the formed silica, which was characterized by the activation energy of the network relaxation; therefore, the moduli of the rubbery state depended on the reinforcement by the formed silica and also depended on the network density.

We could use the hybrid material in this study as a complementary material for conventional thermosetting and thermoplastic resins by taking advantages of its considerable change in modulus around the glass-transition temperature along with its transparency and deformability at high temperatures. In addition, the individual controllability of the glass-transition temperature and the modulus of the rubbery state could be used to design products.

References

1. Wei, Y.; Yang, D. C.; Bhakthavatchalam, R. Mater Lett 1992, 3, 261.
2. Silveira, K. F.; Yoshida, I. V. P.; Nunes, S. P. Polymer 1994, 36, 1425.
3. Tamaki, R.; Chujo, Y. J Mater Chem 1998, 8, 1113.
4. Yeh, J. M.; Weng, C. J.; Huang, K. Y.; Huang, H. Y.; Yu, Y. H.; Yin, C. H. J Appl Polym Sci 2004, 94, 400.
5. Landry, C. J. T.; Coltrain, B. K.; Wesson, J. A.; Zumbulyadis, N.; Lippert, J. L. Polymer 1992, 33, 1496.
6. Nandi, M.; Conklin, J. A.; Salvati, L.; Sen, A. Chem Mater 1990, 2, 772.
7. Morikawa, A.; Iyoku, Y.; Kakimoto, M.; Imai, Y. Polym J 1992, 24, 107.
8. Ruan, S.; Lannutti, J. J.; Prybyla, S.; Seghi, R. R. J Mater Res 2001, 16, 1975.
9. Ravaine, D.; Seminel, A.; Charbouillot, Y.; Vincens, M. J Non-Cryst Solids 1986, 82, 210.
10. Haraguchi, K.; Usami, Y.; Ono, Y. J Mater Sci 1998, 33, 3337.
11. Mauer, B. J.; Liu, D. W.; Jackson, C. L.; Barnes, J. D. Polym Adv Technol 1995, 7, 333.
12. Matějka, L.; Dušek, K.; Pleštil, J.; Kříž, J.; Lednický, F. Polymer 1998, 40, 171.
13. Matějka, L.; Pleštil, J.; Dušek, K. J Non-Cryst Solids 1998, 226, 114.
14. Matějka, L.; Dukh, O.; Kolařík, J. Polymer 2000, 41, 1449.
15. Mauri, A. N.; Riccardi, C. C.; Williams, R. J. J. Macromol Symp 2000, 151, 331.
16. Ochi, M.; Takahashi, R.; Terauchi, A. Polymer 2001, 42, 5151.
17. Ochi, M.; Takahashi, R. J Polym Sci Part B: Polym Phys 2001, 39, 1071.
18. Matsumura, T.; Ochi, M.; Nagata, K. J Appl Polym Sci 2003, 90, 1980.
19. Weng, W. H.; Chen, H.; Tsai, S. P.; Wu, J. C. J Appl Polym Sci 2004, 91, 532.
20. Macan, J.; Ivanković, H.; Ivanković, M.; Mencer, H. J. Thermochim Acta 2004, 414, 219.
21. Lu, S. R.; Hongyu, J.; Zhang, H. L.; Wang, X. Y. J Mater Sci 2005, 40, 2815.
22. Yano, S.; Ito, T.; Shinoda, K.; Ikake, H.; Hagiwara, T.; Sawaguchi, T.; Kurita, K.; Seno, M. Polym Int 2005, 54, 354.
23. Araki, W.; Adachi, T. J Appl Polym Sci 2008, 107, 253.
24. Mascia, L.; Tang, T. J Mater Chem 1998, 8, 2417.
25. Fujiwara, M.; Kojima, K.; Tanaka, Y.; Nomura, R. J Mater Chem 2004, 14, 1995.
26. Pancrazi, F.; Phalippou, J.; Sorrentino, F.; Zarzycki, J. J Non-Cryst Solids 1984, 63, 81.
27. Brinker, C. J.; Tallant, D. R.; Roth, E. P.; Ashley, C. S. J Non-Cryst Solids 1986, 82, 117.
28. Sakka, S. Sol–Gel Science; Agune Shofusha: Tokyo, 1988.
29. Adachi, T.; Sakka, S. J Mater Sci 1990, 25, 4732.
30. Dezhu, M.; Hongjun, C.; Jianbin, Z.; Xiaolie, L. Macromol Chem Phys 1999, 200, 2040.
31. Ueki, T.; Nishijima, S.; Izumi, Y. Cryogenics 2005, 45, 141.
32. Lawrence, E.; Nielsen, L. E. J Macromol Sci Rev Macromol Chem 1969, 3, 69.
33. Lunak, S.; Vladyka, J.; Dusek, K. Polymer 1978, 19, 931.
34. Muller, F. H.; Huff, K. Kolloid Z 1959, 166, 44.